Emerging Quantum-Dots-Enhanced LCDs

Zhenyue Luo, Daming Xu, and Shin-Tson Wu, *Fellow, IEEE*

(Invited Paper)

***Abstract*—Quantum dots (QDs)-based backlight greatly enhances the color performance for liquid crystal displays (LCDs). In this review paper, we start with a brief introduction of QD backlight, and then present a systematic photometric approach to reveal the remarkable advantages of QD backlight over white LED, such as much wider color gamut, higher optical efficiency, enhanced ambient contrast ratio, and smaller color shift. Some popular LC modes are investigated, including twisted nematic, fringing field switching (FFS) for touch panels, multi-domain vertical alignment (MVA) for TVs, and blue phase liquid crystal (BPLC) for next-generation displays. Especially, QD-enhanced BPLC combines the major advantages of FFS and submillisecond response time. It has potential to become a unified display solution.**

***Index Terms*—Blue phase liquid crystal (BPLC), fringe field switching (FFS), liquid crystal display (LCD), quantum dots (QDs).**

I. Introduction

After half a century of extensive material research and device development, followed by massive investment in advanced manufacturing technology, thin-film transistor liquid crystal display (TFT LCD) has become the dominant flat panel display technology [1]. Nowadays, LCDs are ubiquitous in our daily lives; their applications span from smartphones, tablets, computers, large-screen TVs, and data projectors, just to name a few. Recently, there are debates between LCD and organic light emitting diode (OLED) camps: who wins [2]–[5]?

Fig. 1 compares eight performance metrics between in-plane switching (IPS) LCD and RGB OLED for mobile displays. From Fig. 1, LCD is leading in lifetime, power consumption, resolution density and cost; comparable in ambient contrast ratio [3]–[5] and viewing angle, but inferior to OLED in module thickness/flexibility, color and response time. OLED is an emissive device, so its viewing angle, dark state, and module thickness should be superior to those of LCD. However, these gaps are gradually narrowed by the film-compensated multi-domain LC structures, local dimming of backlight (which leads to dynamic contrast ratio over 1,000,000:1), and edge-lit or ultra-thin backlight module (thickness $\sim$ 2 mm) [6]–[8]. The ambient contrast ratios reported by different groups vary slightly [3], [5], but in general they are comparable. The remaining two major challenges for the LCD camp to catch up are response time and vivid colors.

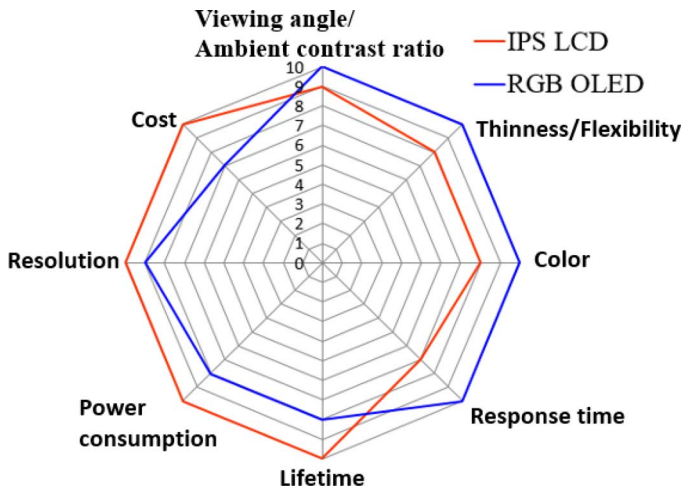

Fig. 1. Performance comparison of in-plane-switching LCD (IPS-LCD) and RGB OLED. (This chart is modified from [4].)

To reduce LC response time, polymer-stabilized blue phase liquid crystal (PS-BPLC) is emerging [9]. Its nano-structure and short coherence length lead to submillisecond response time, which is essential for eliminating image blurs and enabling color sequential display [10]–[12]. With rapid advance in BPLC materials and device structures, the driving voltage has been reduced to $< 10\ V_{rms}$, while maintaining fast response time, high contrast ratio, and negligible hysteresis [13]–[17]. Unlike the current status that fringing field switching (FFS) is favored for touch panels [18]–[21] while MVA (multi-domain vertical alignment) [22], [23] for TVs, IPS-based BPLC merges the advantages of IPS (wide view, weak color shift and pressure resistance) and MVA (high contrast ratio and fast response time) into one. It has potential to offer a total solution for all kinds of display applications, including mobiles and TVs.

Good color performance needs to fulfill a proper white point (for appropriate image shades), wide color gamut (for greater color reproduction range), and ideally no color shift (for better color reproduction accuracy) [8]. A LCD with white LED backlight (blue LED-pumped yellow phosphor) has about 75–80% AdobeRGB color gamut, while commercial OLED covers $\sim$

Manuscript received April 09, 2014; revised May 14, 2014; accepted May 14, 2014. Date of publication May 16, 2014; date of current version May 23, 2014. This work is supported by ITRI, and by AU Optronics, Taiwan. *(Zhenyue Luo and Daming Xu contributed equally to this paper.)*

The authors are with the College of Optics and Photonics, University of Central Florida, Orlando, FL 32816 USA (e-mail: zhenyueluo@knights.ucf.edu; swu@ucf.edu).

Color versions of one or more of the figures are available online at http://ieeexplore.ieee.org.

Digital Object Identifier 10.1109/JDT.2014.2325218

100% AdobeRGB color space [5]. Besides that, LCD has noticeable color shift issue due to angular dependent effective birefringence [8]. To enhance color performance, LCD camp needs to systematically optimize the light source, color filters (CFs), and LC mode.

Several approaches have been proposed to widen the LCD color gamut, but they either sacrifice light efficiency or add more cost. Narrowing the bandwidth of color filters would lead to purer primary colors, but the transmittance is significantly reduced [24]. On the light source side, newly developed white LED with green/red phosphor materials has narrower emission bandwidth, but its efficiency is not yet satisfactory [25]. Discrete RGB LEDs can significantly expand the color gamut, but they require separated driving circuits [26], [27]. In addition, the availability of high efficiency green LED remains a challenge, which is known as green gap.

Recently, a promising new backlight technology involving quantum dots (QDs) is emerging [28]–[32]. It uses blue LED to excite the green/red QD mixture. The full emission spectrum consists of three well-separated peaks, corresponding to three highly saturated primary colors. Several companies are actively engaged into this area, including material providers (Nanosys, QD vision, Nanoco), device developers (3M, Pacific Lighting) as well as TV manufacturers (Samsung, LG, Sony, Amazon) [33]–[38]. As a matter of fact, Amazon has recently introduced Kindle Fire HDX 7 and Sony introduced Triluminos TV with QD-enhanced backlight.

In this review paper, we present the recent progress and remaining challenges related to QD-enhanced LCDs. In comparison with white LED, QD backlight exhibits following advantages: higher light efficiency ($\sim$ 15%–20%), wider color gamut (115% AdobeRGB in CIE 1931 and 140% in CIE 1976 color space), excellent color purity under ambient condition, and smaller color shift. Two QD-based LCD systems are used as examples here: 1) by integrating QD backlight with FFS mode [21], [39]–[43], we can achieve high optical efficiency, wide viewing angle, and vivid colors for mobile displays and 2) by integrating QD backlight with IPS-based blue phase LCD, we can achieve vivid color and submillisecond response time for both mobile displays and TVs.

II. Basics of QD Backlight

QDs are semiconductor nanocrystals with diameter of 2 $\sim$ 10 nm. As the electrons and holes are confined in such small particles, quantum confinement effects dominate their physical properties [44]. Fig. 2 depicts the bandgap diagram of QDs. Unlike bulk material, the energy levels of QDs are discrete and affected by both material property and particle size. The system can be described by a finite quantum well problem, and the effective bandgap that determines the energy (and hence color) of the fluorescent light can be approximated by Brus equation [45]:

$$E^* \cong E_g + \frac{\hbar\pi^2}{2R^2}\left[\frac{1}{m_e} + \frac{1}{m_h}\right] \quad (1)$$

where E_g is the bandgap of bulk semiconductor, R is the particle radius, and m_e and m_h are effective mass of electron and hole, respectively. From (1), the QD's optical properties can be varied by changing the particle size. For example, when using an ultraviolet light to excite CdSe QDs with different particle sizes, the fluorescence color can cover the entire visible range. A larger R leads to a longer wavelength emission. For industrial application, finding a high quality fluorescent material at certain wavelength could be challenging. For example, green inorganic semiconductor materials have relatively low quantum efficiency, while blue emissive organic materials have low efficiency as well as limited device lifetime. QDs enable us to obtain any specific color emission via varying the particle size while using the same material system. This property opens a new design freedom. For example, we can engineer QD's emission spectrum to match with color filters for boosting optical efficiency and widening color gamut simultaneously.

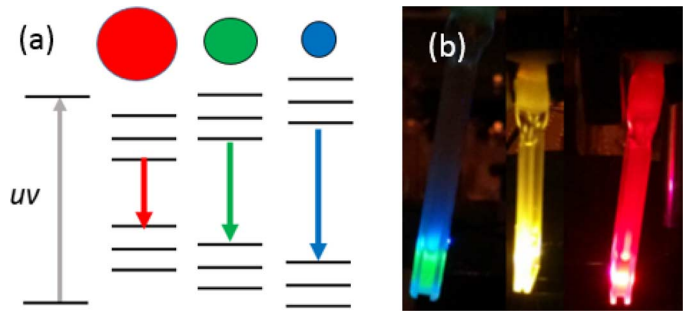

Fig. 2. (a) Illustration of QD bandgap diagram. (b) Vivid fluorescent colors when QDs with different sizes are excited by an UV light.

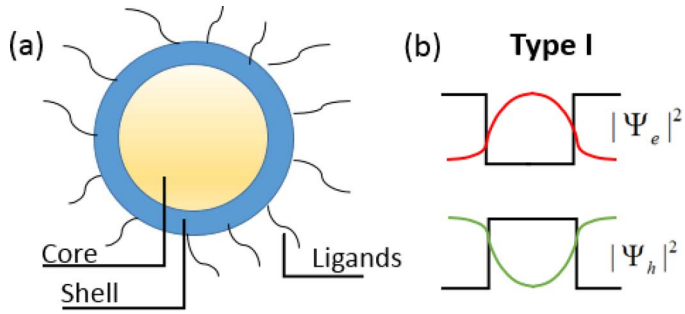

Fig. 3. (a) Structure of core-shell QD. (b) Bandgap diagram of type-I core-shell QD.

Another desirable feature of QDs is their high-purity emission colors. The emission of a QD sample is the convolution of fluorescence emission of each individual QD in a population. Therefore, the line-width is determined by inhomogeneous broadening of QD particle size distribution. Current chemical synthesis techniques manifest excellent controllability over particle size distribution, it can provide batches of QDs containing $> 10^{19}$ particles that are all within ± 1 atom of thickness variation [37]. The full width half maximum (FWHM) of Cd-based QDs is around 30 nm. Moreover, new colloidal particles in the form of platelets show 10-nm FWHM [46], [47]. Such a narrow emission line-width would undoubtedly produce an exceedingly wide color gamut.

To enhance quantum efficiency and material stability, QDs used for display and lighting usually have Type-I core-shell structure and organic ligands [48], [49]. Fig. 3(a) shows the core-shell structure: the core QD is covered by a shell with larger band gap, and then surrounded by organic ligands.

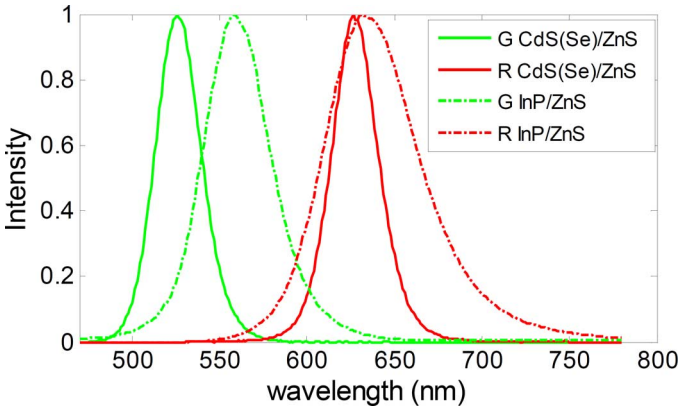

Fig. 4. Normalized emission spectrum of green/red CdS(Se)/ZnS QDs (solid lines) and green/red InP/ZnS QDs (dashed lines).

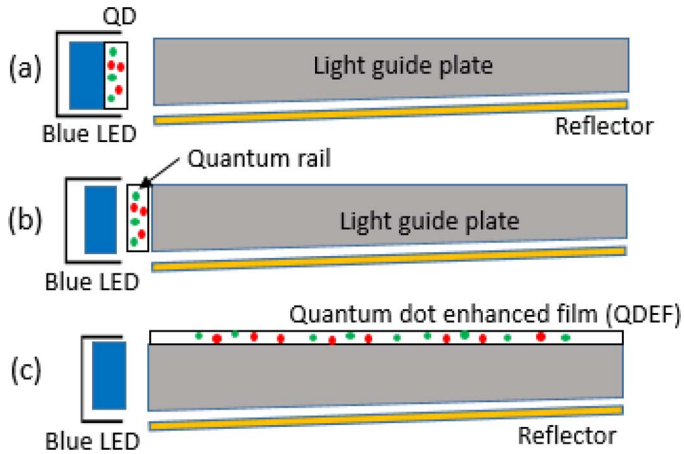

Fig. 5. Three different QD backlight geometries. (a) QD is included in the LED dome. (b) QD is on the edge of light guide plate, called quantum rail. (c) QD is on the top surface of light guide plate, called QDEF.

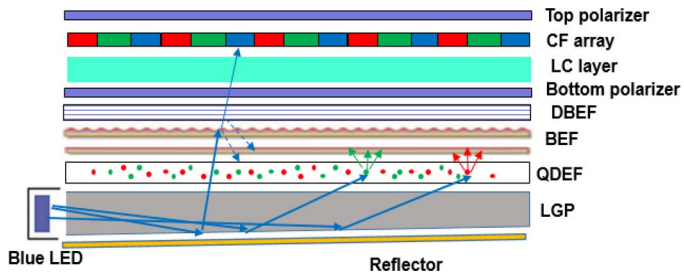

Fig. 6. A typical LCD system with QDEF structure.

The organic ligands provide excellent surface passivation and eliminate deleterious surface states [29], [49]. The core-shell structure effectively confines the wavefunction of exciton within the core [Fig. 3(b)], which leads to high recombination rate and enhanced emission quantum efficiency. As a matter of fact, Cd-based QD materials have been found with $> 95\%$ quantum efficiency and 30 000 hours of lifetime [36].

Various QD materials have been synthesized and studied, including II–VI semiconductors (ZnS, CdSe, CdS, ZnSe), III–V semiconductors (InP), ternary semiconductors $(CuInS_2)$, and doped material (ZnSe:Mn) [50]–[53]. Among them, Cd-based QDs are most popular for display and lighting applications due to their high quantum efficiency $(> 95\%)$ and narrow linewidth (FWHM $\sim$ 30 nm). However, Cd is toxic and is regulated by several countries. Recently there are intensive efforts to seek a non-Cd replacement. Among all the alternative materials, InP based QDs are the most promising candidates, whose quantum efficiency is comparable to the best performing CdSe QDs, but its emission linewidth is somewhat broader [51]. Fig. 4 shows the normalized emission spectrum of four QD materials. The Cd-based QDs exhibit a $\sim$ 30-nm FWHM, while the InP QDs is $\sim$ 50 nm. Two reasons account for this broadening spectrum: 1) the chemical synthesis method of InP QDs is not yet mature enough and 2) the quantum confinement effect in InP QDs is much stronger, therefore InP emission is more susceptible to particle size variation [50]. InP QDs will be more attractive for display once their FWHM can be further reduced.

Both electroluminescence (EL) and photoluminescence (PL) have been developed for display applications. In EL mode, the QDs are activated by electronic energy to directly emit colored lights [31], [32]. Its working principle is very similar to that of OLED. As a result, the EL QD is termed as quantum-dot light emitting diodes (QLED). Although the QLED performance is rapidly improved in recent years, it may still take several years to fully compete with OLED [54].

In PL devices, QDs are usually pumped by a UV lamp or an InGaN blue LED. Here, QDs play a similar role to conventional phosphors, but with more design freedom and better color purity. The PL mode only involves pure optical process and has a relatively simple structure. Such a QD device is cost effective and reliable, thus, it is ready for commercial applications.

QDs can be dispersed in a polymer matrix, processed with existing optical film technique, and conveniently integrated with current LCD backlight system. As Fig. 5 depicts, there are three likely choices to implement QD [34]: 1) on LED chip [33]; 2) on the edge of light guide plate (LGP), known as 'Quantum rail' or 'Color IQ' by different companies [36]; and 3) on the top surface of LGP as a film, called "quantum dot enhanced film (QDEF)" [35]. Among the three configurations, the on-chip approach consumes minimum amount of QD materials. Nevertheless, QDs encapsulated on-chip would operate at high temperature ($\sim$ 150 °C) and exposed to intensive light excitation. This may significantly decrease QD's quantum efficiency and lifetime. Packaging problem and material reliability must be solved before on-chip approach can be widely applied. The amount of material needed for quantum rail and QDEF scales with display sizes. QDEF consumes a lot more QD material than Quantum rail. Therefore, QDEF is more favorable to small panels while Quantum rail is more attractive to large panels. As a matter of fact, Amazon's 7.9" Kindle Fire HDX uses QDEF while Sony's 65" Triluminos TV uses Quantum rail.

Fig. 6 plots a typical LCD system with QDEF structure. It consists of a blue LED array, LGP to steer the light source toward the TFT-LCD panel, QDEF, a series of optical films, and polarizers [55]. Blue LEDs are placed on the edge of the LGP. The blue light travels in the LGP and coupled out by specifically designed micro extractors. The emerging blue light excites the green/red QDs dispersed in the QDEF. Once the excited electrons relax back to their ground states, QDEF emits green

and red lights. Brightness enhancement films (BEFs) and Dual Bright Enhance Films (DBEFs) play a significant role in balancing the angular distribution of blue LED light and green and red QD lights. Therefore, color uniformity at different viewing angle can be maintained. BEFs and DBEFs also introduce light recycling and enhance the effective optical path length within the QDEF. This helps to reduce the QD density and avoid QD aggregation and quenching. As a result, QDEF has an excellent device reliability ($>$ 30 000 hours) [38].

III. Optimization of QD Backlight

The unique properties of QD make it attractive as LCD backlight. Fig. 7(a) compares the emission spectrum of QD backlight and conventional white LED with one yellow phosphor (1p-LED). 1p-LED has a sharp emission peak from blue LED with a 20-nm FWHM. However, the fluorescence from YAG:Ce yellow phosphor is fairly broad (FWHM $\sim$ 130 nm). The light source itself does not exhibit separated emission bands for green and red. Thus, the color performance totally relies on the color filters. Fig. 7(b) shows the light spectrum after passing through color filters; the green and red color primaries are still not saturated and there is significant color crosstalk. On the other hand, QD backlight remains three separated and narrow bands. Each emission band can be designed to match the transmission peaks of the employed color filters for increasing light output. Fig. 7(c) depicts the color space of the Commission Internationale de l 'Eclairage (CIE) 1931. The 1p-LED has 79% AdobeRGB color gamut, while the QD backlight covers $\sim$ 120% color area. Therefore, QD not only widens color gamut but also improves optical light efficiency.

Since QD backlight provides an extra design freedom in selecting a desired emission spectrum, we can take this advantage to optimize the system performance. QDs partially absorb the incident blue light and down-convert it to green and red. The total emission consisting of three peaks and spectral power distribution (SPD) can be described as:

$$S_{\text{in}}(\lambda) = f_b S(\lambda, \lambda_b, \Delta\lambda_b) + f_{\text{g}} S(\lambda, \lambda_{\text{g}}, \Delta\lambda_{\text{g}}) + f_r S(\lambda, \lambda_r, \Delta\lambda_r) \quad (2)$$

where $\mathrm{S}(\lambda, \Delta\lambda_i, f_i)$ $(i = r, \mathrm{g}, b)$ is the Gaussian function used to fit the emission spectra of blue LED and green/red QDs, and λ_i, $\Delta\lambda_i$, and f_i represent the central wavelength, FWHM, and relative intensity, respectively.

Such a discrete three color spectrum is very ideal for LCD. Fig. 8 depicts the light flow chart in a typical LCD panel. The incident light $S_{\text{in}}(\lambda)$ is split into three channels: red (R), green (G) and blue (B) corresponding to the color filters. The TFT aperture ratio, LC layer, applied voltage, and color filters jointly determine the optical efficiency and color saturation of a LCD panel. The three light channels finally mix together and transmit out of the LCD panel with SPD $S_{\text{out}}(\lambda)$ given as

$$\begin{aligned} S_{\text{out}}(\lambda) &= S_{\text{out},R}(\lambda) + S_{\text{out},G}(\lambda) + S_{\text{out},B}(\lambda) \\ &= S_{\text{in}}(\lambda) P(\lambda) R(\lambda) LC(V_1, \lambda) A_R \\ &\quad + S_{\text{in}}(\lambda) P(\lambda) G(\lambda) LC(V_2, \lambda) A_G \\ &\quad + S_{\text{in}}(\lambda) P(\lambda) B(\lambda) LC(V_3, \lambda) A_B. \end{aligned} \quad (3)$$

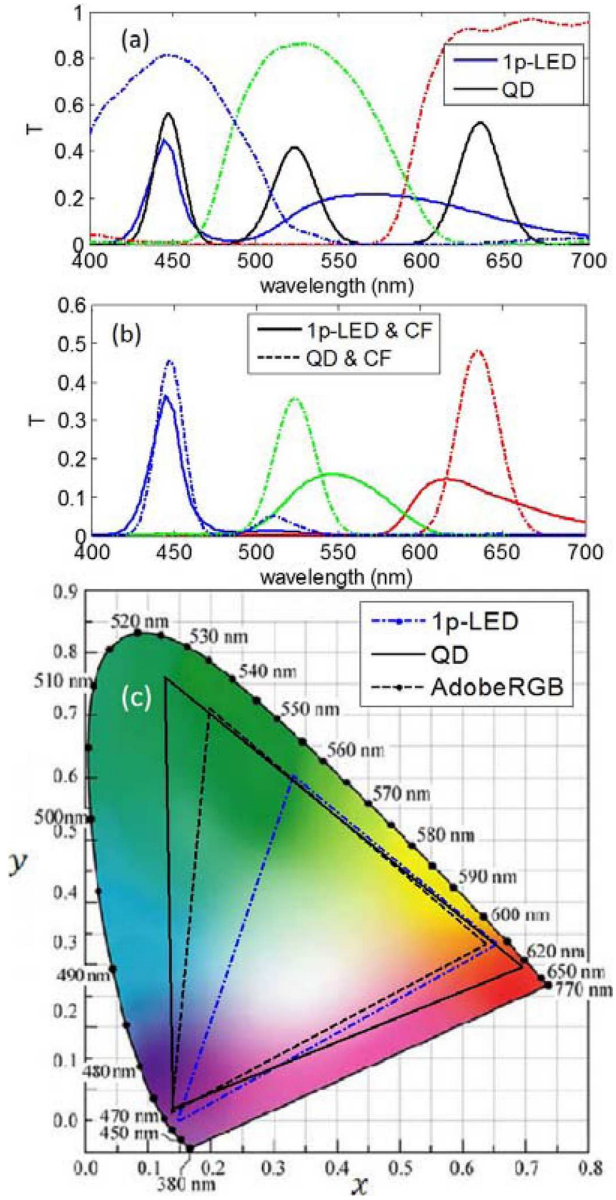

Fig. 7. (a) Transmission spectra of color filters and emission spectra of QD backlight and 1p-LED. (b) The transmitted spectrum after passing through color filters. (c) the simulated color gamut in CIE 1931.

Two metrics are defined here to evaluate the backlight performance:

1) Total Light Efficacy (TLE):

$$\text{TLE} = \frac{683 \frac{\text{lm}}{W_{\text{opt}}} \int S_{\text{out}}(\lambda) V(\lambda) d\lambda}{\int S_{\text{in}}(\lambda) d\lambda}. \quad (4)$$

It represents how much input light is transmitted through the LCD panel and finally converted to the brightness perceived by human eye. To calculate TLE, we need to consider the human eye sensitivity function $V(\lambda)$. It is centered at $\lambda = 555$ nm, meaning human eyes are more sensitive to green/yellow light [56]. TLE measures the backlight's total efficiency; it considers almost every factor in the display system, such as light source spectrum, transmittance of color filters, LC layer and polarizers,

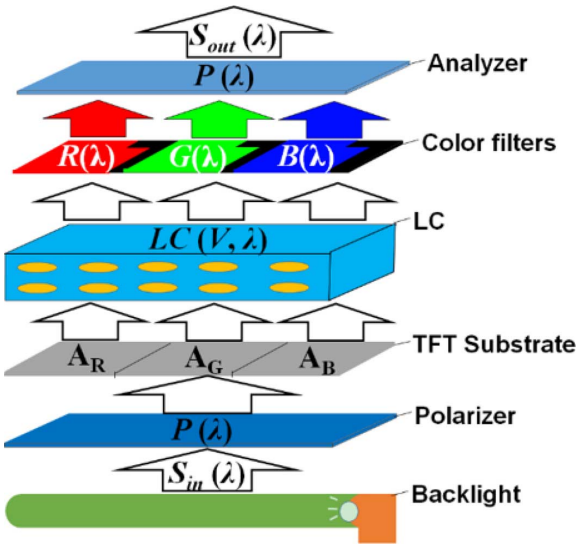

Fig. 8. Light flow chart in a typical LCD system.

aperture ratio of each light channel, as well as human eye sensitive function.

2) Color Gamut:

$$\text{Color gamut} = \frac{\text{Area encicled by RGB primaries}}{\text{Area defined by AdobeRGB standard}}. \quad (5)$$

It indicates the range of colors that can be faithfully reproduced by the LCD. Color gamut can be defined either in CIE 1931 or CIE 1976 color space. Although CIE suggests using CIE 1976 definition since it is much more color uniform, many companies and research groups are still using CIE 1931 to evaluate their products [35]. To satisfy both camps, later we will present color gamut in both CIE 1931 and CIE 1976. Further information regarding different color spaces can be found in [57].

A backlight with optimal $P_{\text{in}}(\lambda)$ should achieve a large color gamut while maintaining high *TLE*. As an example, we fix the proportion of each color component (f_r, f_g, f_b) to obtain the display white point at D65 ($x = 0.312$, $y = 0.329$ in CIE1931 color diagram) [56]. The remaining free parameters are central wavelength and FWHM of each color component. In total, there are $3 \times 2 = 6$ free parameters and two metric functions that are subject to optimization:

$$\begin{aligned} \text{Color gamut} &= F_1(\lambda_b, \Delta\lambda_b, \lambda_g, \Delta\lambda_g, \lambda_r, \Delta\lambda_r), \\ \text{TLE} &= F_2(\lambda_b, \Delta\lambda_b, \lambda_g, \Delta\lambda_g, \lambda_r, \Delta\lambda_r). \end{aligned} \quad (6)$$

For practical considerations, we also set the following constraints: 400 nm $< \lambda_b <$ 500 nm, 500 nm $< \lambda_g <$ 600 nm, 600 nm $< \lambda_r <$ 700 nm, 20 nm $\leq \Delta\lambda_b \leq$ 30 nm, 30 nm $\leq \Delta\lambda_g, \Delta\lambda_r \leq$ 50 nm. For such a multi-objective problem, we chose the particle swarm optimization algorithm [58], [59] to search for the optimal solution and found there is no single result that can co-maximize the above two objective functions. Instead, we obtained a group of solutions; improvement of one objective is compromised by the degradation of another objective. This group of solutions forms the so-called *Pareto front*.

We first analyze the color performance of a mobile display using fringing field switching with a negative $\Delta\varepsilon$ liquid crystal

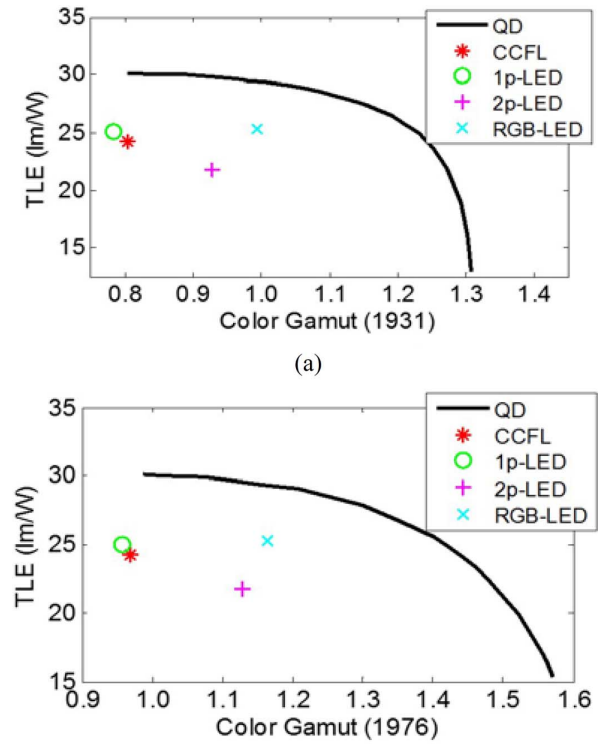

Fig. 9. TLE versus color gamut in: (a) CIE 1931 and (b) CIE 1976 color space. LCD mode: n-FFS. White Point: D65. Black solid lines represent the Pareto front of QD backlight.

(n-FFS). Since color gamut can be defined either in CIE 1931 color space or CIE 1976 color space, we performed two separate optimizations and the results are shown in Fig. 9(a) and 9(b), respectively. The QD backlight could vary from low color gamut (80% AdobeRGB) but high *TLE* (30.2 lm/W) to high color gamut (130% AdobeRGB) but low *TLE* ($<$ 20 lm/W). The tradeoff between *TLE* and color gamut cannot be avoided since the two objectives are intrinsically exclusive. To enhance light efficiency, the three emission peaks should be located close to 550 nm where human eye is most sensitive; while for the purpose of extending color gamut, the emission peaks should be well separated in order to reduce color crosstalk [58]. Given the series of solutions, for different application needs, we can select the most suitable solution among those according to the different system requirements of light efficiency and color gamut.

The performances of conventional backlight sources are also included in the same figure for comparison, including: 1) cold cathode fluorescent lamp (CCFL); 2) single-chip white LED with yellow phosphor (1p-LED); 3) single chip white LED with green and yellow phosphor (2p-LED); and 4) multi-chip RGB LEDs (RGB-LED). The emission spectra are obtained from [8] and [25]. In terms of energy efficiency and color gamut, RGB LEDs seem to be the optimal solution, yet it requires complicated driving circuits and is not cost effective. From low cost perspective, WLED based on blue LED-pumped phosphorescence is still a favored choice among the conventional backlight sources.

From Fig. 9(a), it is evident that QD backlight has superior performance to conventional backlights. For example, by

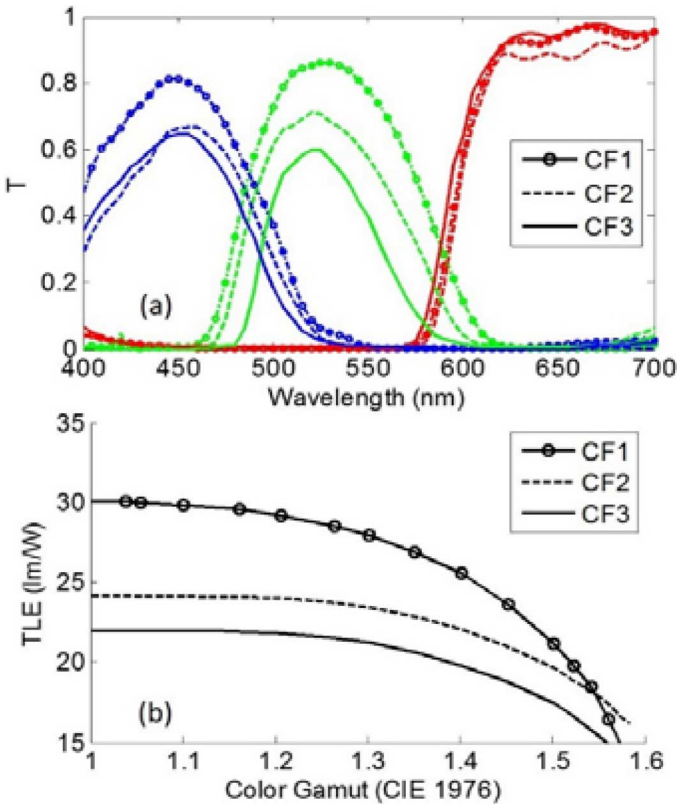

Fig. 10. (a). Transmission spectrum of different color filters. (b) Pareto front of TLE and color gamut for different color filters. LCD mode: n-FFS. White Point: D65.

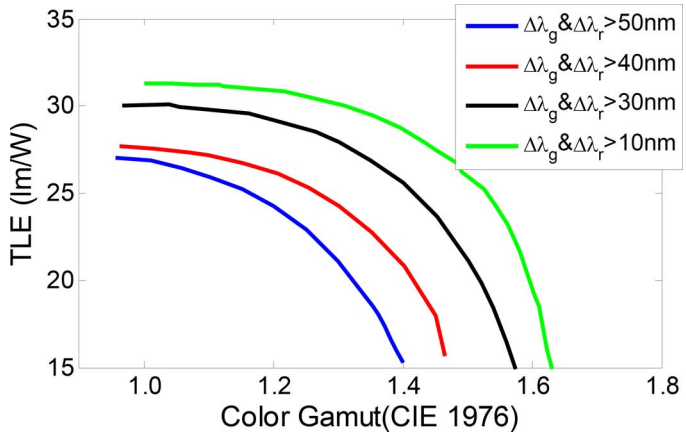

Fig. 11. *Pareto front* of TLE and color gamut for QD with different FWHM lower limits.

keeping the same TLE as that of RGB LEDs, the QD backlight can achieve 121% color gamut, which is much larger than that of any conventional backlights. Similarly, by keeping the same color gamut as RGB LEDs, the QD backlight can achieve TLE $\sim$ 29.2 lm/W, which is $\sim$ 15% higher than that of RGB LEDs (25.3 lm/W).

According to Fig. 9(b), the color gamut defined in CIE 1976 color space is correspondingly higher. By keeping the same TLE as that of RGB LEDs, the QD backlight can $>$ 140% color gamut. This is a tremendous improvement compared to conventional backlights and also significantly larger than that of commercial OLED color gamut ($\sim$ 100%).

Besides backlight source, color filters also play an important role in determining LCD's color performance [24], [27]. Fig. 10(a) shows the transmission spectra of three commercial color filters. CF1 has the highest transmission peak but it has significant overlap in the blue-green and red-green regions. To reduce color crosstalk, CF2 and CF3 employ green photoresist with a narrower FWHM but their transmittance is sacrificed. With proper combination of CF3 and 2-p WLEDs, the LCD can cover the whole AdobeRGB region [24]. However, this method sacrifices the \CF transmission and therefore the display device is less energy efficient.

For comparison, we optimized QD backlight for different CFs and results are shown in Fig. 10(b). QD backlight with CF1 has the highest light efficiency and significant color gamut. CF2 and CF3 improve the color gamut slightly, but they drastically reduce the system light efficiency. Narrow band color filters are not effective for QD backlight, especially when considering the loss in light efficiency. It is because QD backlight itself has very pure emission peaks and is less dependent on the color filters. As a result, QD backlight mitigates the color separating requirement for CFs. By using broadband CFs, the cost can be reduced and the optical efficiency can be further improved.

The FWHM of QD emission greatly affects the display performance. During previous calculations, we considered Cd-based QD and set a lower limit on FWHM, namely $\Delta\lambda_g$ & $\Delta\lambda_r \geq 30$ nm. However, for non-Cd QD (for example, InP) the FWHM is larger [51]. Fig. 11 depicts the performance of QDs with different FWHM lower limits. As the lower limit of $\Delta\lambda_g$ and $\Delta\lambda_r$ increases from 30 nm to 50 nm, both color gamut and TLE are reduced. This is understandable since a broader emission band leads to less saturated color primary and narrower color gamut. In order to compensate this effect, the three emission bands should be well-separated, so TLE will decrease. In general, narrower QD emission is always preferred for a high performance backlight. Non-Cd QDs need to enhance color purity in order to match the performance of Cd-based QDs. Recently platelet QDs show $\sim$ 10-nm FWHM [46], [47]. This material can further improve the display performance and build unbeatable advantages for QD backlight.

In a LCD, the white point is obtained when all the pixels are at their maximum grey levels, and the corresponding color temperature is between 6000 K and 10000 K. However, during manufacture process the white point may not occur at the desired color coordinates, resulting in unnatural colors. The white point can be corrected by reverse engineering. Several approaches can be applied to balance the RGB output and achieve the desired white point: 1) varying the aperture ratio of RGB primaries (A_R, A_G, A_B); 2) optimizing the LC cell gap for a proper wavelength; and 3) tuning the backlight emission spectrum. The first approach adds complexity to the manufacture process, while the second approach usually compromises the transmittance for the G and R channels. In QD backlight, we can readily tune the QD concentration to achieve the desired white point. In fact, the selection of white point also affects the LCD performance. Fig. 12 shows the *Pareto front* when the white point is set at different color temperatures. A lower color temperature white point will

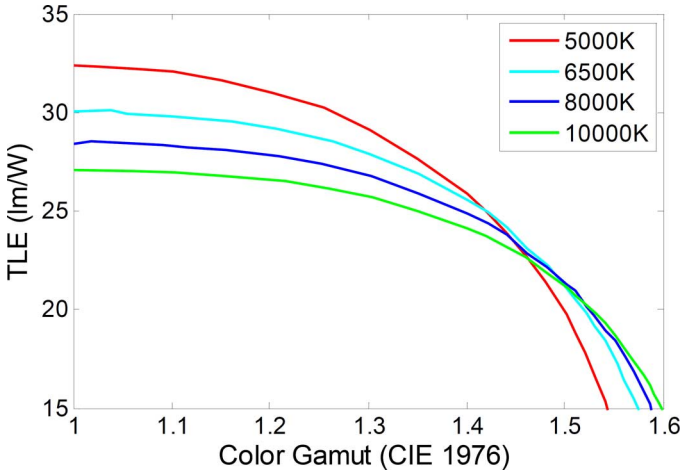

Fig. 12. *Pareto front* of TLE and color gamut for QD enhanced LCD with different white point.

result in higher light efficiency but limited color gamut, while a higher color temperature white point will result in a wider color gamut with reduced light efficiency. A proper selection of white point should balance both light efficiency and color gamut.

As a summary of this section, QD backlight brings several advantages to LCDs. 1) Their narrow emission spectra lead to vivid colors and large color gamut ($\sim$ 120% in CIE 1931 and $\sim$ 140% in CIE 1976). 2) The LCD system light efficiency can be improved by $\sim$ 15% by optimizing QD emission spectrum to match with color filters. 3) QD backlight mitigates color separating requirement of color filters. By using broadband CFs, the cost can be reduced and the system light efficiency improved. 4) QD spectrum can be readily designed for different application needs, such as achieving different white point. In fact, QD backlight can also be integrated with multi-color primary technique to further improve display performance [60]. In next section, we will combine the QD backlight with some advanced LC modes and systematically evaluate the display performance.

IV. QD-Enhanced LCDs

A. Different LC Modes

The applications of LCD range from smartphones, tablets, computers, to large-screen TVs, and data projectors. Besides general requirement needs such as high resolution, fast response time, vivid color etc., different applications put different performance preference on LCD products: Mobile display prefers low energy consumption (to extend battery life), and pressure-resistance (for touch screen), while large screen TV favors large viewing angle (for multi-viewer) and excellent contrast ratio (for image quality). Several LCD modes are developed to fulfill different application requirements.

Table I compares four popular LC modes:

1) *TN mode [61]:* It uses longitudinal field to unwind the twisted LC directors. This mode has simple structure and high transmittance, yet its viewing angle is somewhat limited. Currently TN is mostly used in displays that do not require high image quality, such as wristwatches, signage, as well as laptop computers.

TABLE I
Comparision of Different LCD Modes

	TN	MVA	IPS & FFS	IPS-BPLC
Contrast ratio	Fair	Excellent	Good	Good
Transmittance (relative to TN)	100%	~70%	IPS~70% p-FFS~88% n-FFS~95%	~80%
Viewing angle	Fair	Good	Excellent	Excellent
Color shift	Fair	Good	Excellent	Excellent
Response time	~20 ms	~5 ms	~20 ms	<1 ms
Touch insensitivity	No	No	Yes	Yes
Potential to color sequential	No	No	No	Yes

2) *MVA mode [22], [62]:* LC molecules are initially vertically aligned in the voltage-off state. Upon applying a voltage, the longitudinal electric field controls the LC tilt angle to display different grey levels. This mode has highest on-axis contrast ratio and relatively fast response time, and is most favorable for large screen TVs. However, its color shift at off-axis is still noticeable.
3) *IPS mode and FFS mode [20], [41], [43]:* LC directors are homogenously aligned and parallel to the optical axis of the polarizer in the voltage-off state. Upon applying a voltage, the transversal electric fields reorient the LC mainly in the same plane which in turns causes phase retardation to the incident beam for displaying gray levels.
In IPS mode, the LC molecules above the electrodes cannot be effectively rotated. These 'dead zones' lower the transmittance to $\sim$ 70% [23]. In FFS mode, the fringe field covers both electrode and gap regions, so that there is no dead zone [21]. Both positive (p-FFS) and negative (n-FFS) $\Delta\varepsilon$ LCs can be used in FFS mode; p-FFS can achieve 88% transmittance, while n-FFS can achieve 98%. Among all the LCD modes, FFS has the best pressure-resistance [18], [19] and therefore it is widely employed for mobile displays.
4) *IPS-based IPS-BPLC:* This mode uses polymer-stabilized BPLC. In the voltage-off state, the BPLC medium appears optically isotropic, leading to a very good dark state. When an electric field is applied, the induced birefringence is along the electric field direction. Macroscopically, such an isotropic-to-anisotropic transition can be described by the extended Kerr effect [17]. The response time of BPLC is in the submillisecond range [63].

In principle, QD backlight can be applied to all display modes. In Fig. 13, we compare the *Pareto front* of QD backlight for five LCD modes. The device structures and material properties of TN, IPS and MVA can be found in [58], while FFS structure will be defined later. For all the employed LC modes, QD backlight promises a very wide color gamut ($>$ 140%) in CIE 1976 color space, but the actual optical efficiency depends on the LC mode. As shown in Fig. 5, different QD backlight configuration can be used to fit different panel sizes.

In comparison with MVA, IPS, and p-FFS, n-FFS shows a much higher light efficiency. Although its transmittance is

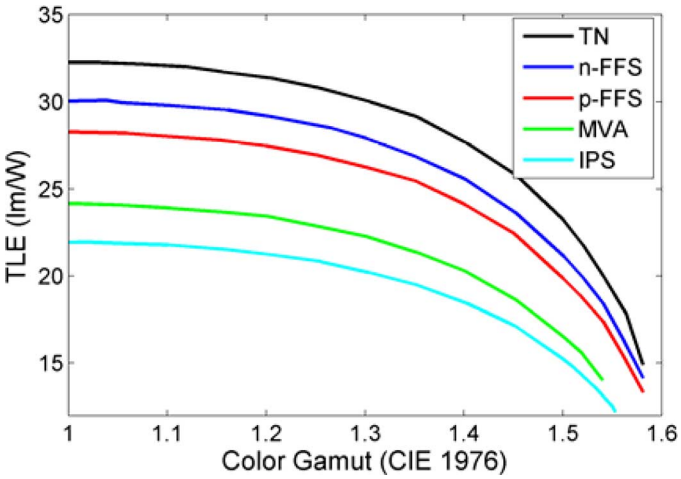

Fig. 13. *Pareto front* of TLE and color gamut for different LC modes.

slightly lower than that of TN, the passivation layer in n-FFS serves as a built-in storage capacitor so that its TFT aperture ratio is higher than that of TN. After considering the aperture ratio effect the overall light efficiency of n-FFS is comparable to that of TN, but with wider viewing angle.

Recently, significant progress has been made in FFS and BPLC modes. Here, we demonstrate that these two modes can also benefit from QD backlight for achieving radiant colors.

B. QD-Enhanced FFS LCD

Currently, p-FFS mode is widely employed in mobile displays, such as iPhone and iPad. The primary reason is that it is relatively easy to obtain a large $\Delta\varepsilon(\sim 10)$ nematic LC while keeping a low viscosity. Large $\Delta\varepsilon$ helps to reduce operation voltage while low viscosity helps to shorten response time. However, p-FFS displays exhibit some shortcomings: 1) the peak transmittance is limited to $\sim 88\%$; 2) the voltage-dependent transmittance (VT) curves do not overlap well for RGB colors, so it requires separate driving circuits for each color; and 3) small but noticeable image flickering due to flexoelectric effect [64].

To overcome these drawbacks, n-FFS LCD has been proposed. It exhibits some superior performances to conventional p-FFS [39], [40]. Fig. 14 compares the VT curves for these two modes. The n-FFS shows following attractive properties: 1) its peak transmittance reaches $\sim 98\%(\lambda = 550$ nm) at $V_{\rm on} = 6.1$ V. 2) RGB colors have nearly the same $V_{\rm on}$. The inset of Fig. 14 depicts the normalized VT curves and they overlap amazingly well. Thus, a single gamma curve driving can be realized for n-FFS, which would simplify the driving circuit.

To improve off-axis image quality, we insert one layer of half wave biaxial compensation film to enlarge the viewing angle [65], [66]. Fig. 15 shows the isocontrast plots. Both p-FFS and n-FFS can achieve a contrast ratio over 100:1 in almost the entire viewing zone $(\pm 85^\circ)$. To further improve off-axis contrast ratio, multi-domain structures can be considered.

Grayscale inversion is another important concern for a display device. Here, we compare grayscale inversion of the *single-domain* n-FFS and p-FFS. Fig. 16(a) and 16(b) shows

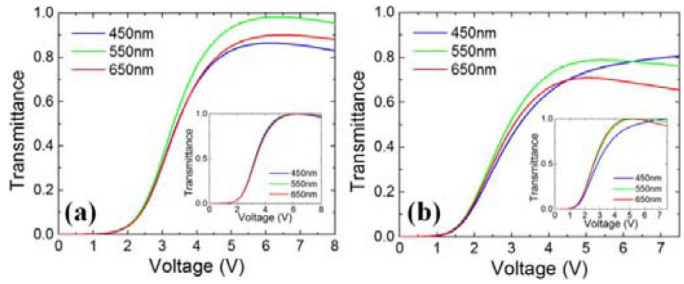

Fig. 14. VT curves for (a) n-FFS using MLC-6882 and (b) p-FFS using MLC-6686. The inset plots show the normalized VT curves. FFS cell: electrode width $w = 2$ μm and electrode gap $l = 3.5$ μm. Cell gap are optimized at $\lambda = 550$ nm with $d\Delta n \sim 360$ nm for n-FFS and ~ 380 nm for p-FFS.

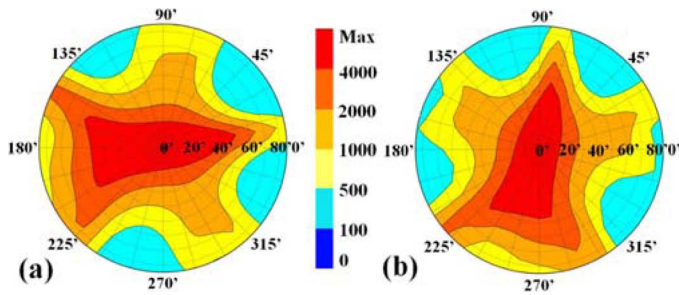

Fig. 15. Isocontrast plots of biaxial-film-compensated (a) n-FFS and (b) p-FFS ($\lambda = 550$ nm).

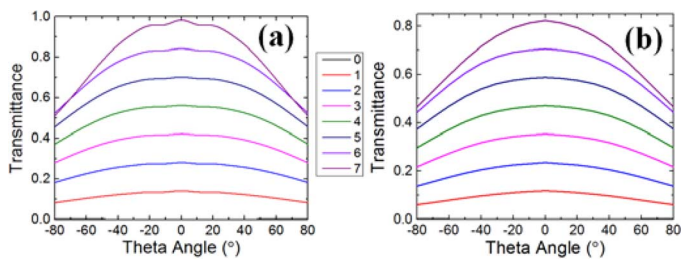

Fig. 16. Viewing angle dependence of the eight gray levels for film-compensated single-domain (a) n-FFS and (b) p-FFS along the diagonal direction ($\phi = 45^\circ$).

the viewing angle dependent eight gray levels for film-compensated n-FFS and p-FFS according to the polar angles in the diagonal direction, in which the grayscale inversion is the worst. From Fig. 16(b), grayscale inversion is not observed in p-FFS mode, whereas a tiny inversion occurs between the 7th and the 8th gray levels in n-FFS mode when the theta angle is larger than 70°. Fortunately, this small grayscale inversion occurs at high gray levels (bright states), which is more difficult to detect by human eyes than low gray levels. Human eyes are more sensitive to the grayscale inversion at low gray levels.

To further compare the grayscale inversion between n-FFS and p-FFS, we convert the transmittance data into gamma curves according to $\mathrm{T} = (\mathrm{GL}/255)^{2.2}$, where GL stands for gray level. All the gray levels were considered (G0-G255) and the gamma curves of n-FFS and p-FFS are plotted in Fig. 17. The most severe grayscale inversion occurs at G248, with 109.47% transmittance. For p-FFS, the grayscale inversion is less severe, as the largest inversion occurs at G250 with a 105.41% transmittance. To more quantitatively evaluate the

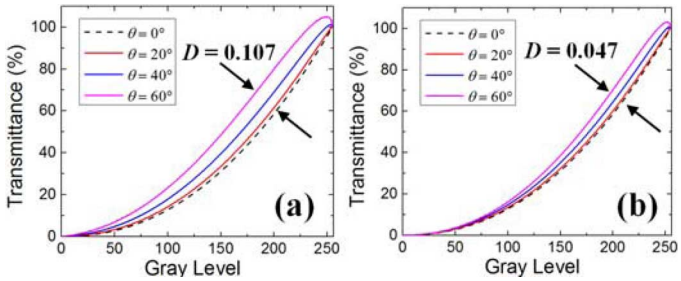

Fig. 17. Viewing angle dependence of gamma curves for film-compensated single-domain (a) n-FFS and (b) p-FFS along the diagonal direction. ($\phi = 45°$).

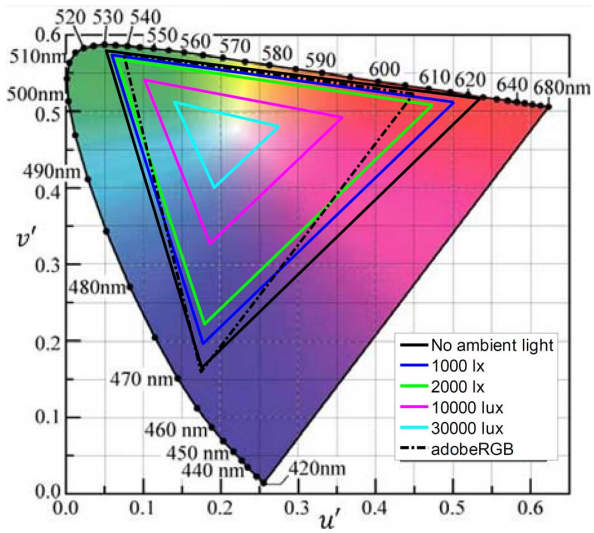

Fig. 18. Variation of display color gamut at different ambient light levels. The LCD is assumed to have luminance intensity of 500 cd/m^2 and 5% surface reflection.

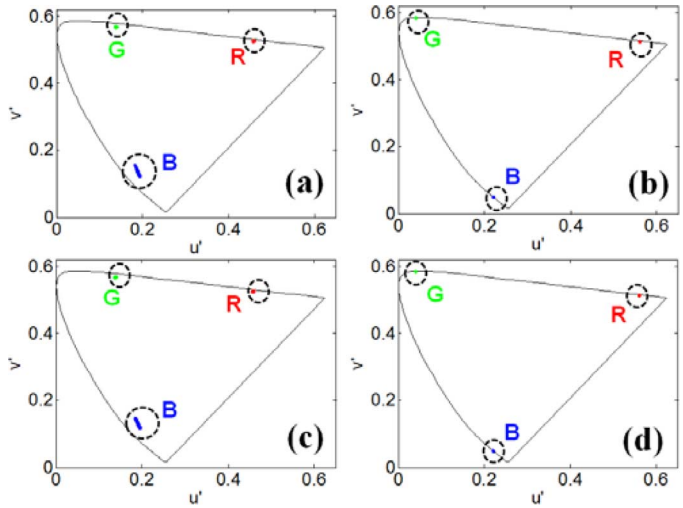

Fig. 19. Color shift of RGB primaries in the film-compensated single-domain FFS at 70° incident angle: (a) n-FFS using white LED, (b) n-FFS using QD-LED ($\Delta\lambda = 10$ nm), (c) p-FFS using white LED, and (d) p-FFS using QD-LED ($\Delta\lambda = 10$ nm). In the simulations, we fix the incident angle of the RGB primaries at 70°, while scanning the azimuthal angle ϕ across the entire 360° at 10° step. Calculations are performed following the route in [8], [71].

grayscale inversion, we used the off-axis image distortion index $D(\theta, \phi)$, defined in [67]. Our simulations show that n-FFS and p-FFS modes have D values of 0.107 and 0.047, respectively. Although the grayscale inversion in n-FFS is slightly worse, it is still much superior to other conventional LCD modes, such as TN and MVA [43]. Moreover, multi-domain FFS structures can be used to further suppress gray level inversion.

Besides the above-mentioned features, QD backlight makes n-FFS more appealing from color aspect:

1) Superior Image Quality at Outdoor Environment: Sunlight readability is an important issue for mobile displays. As the ambient light flux increases, the displayed image could be washed out [5], [68]. The reflected ambient light degrades color characteristics because a portion of the reflected light is also seen as noise by the observer. For an LCD with 1p-LED backlight, the color gamut is 95% AdobeRGB at dark room (0 lux), but is reduced to 77% and 70%, respectively, at 1000 lux (very bright indoor lighting) and 2000 lux (outdoor daylight in heavy shade). The reduced color gamut deteriorates image quality. Fig. 18 depicts the color gamut of QD-enhanced n-FFS LCD under different ambient light levels. Although the color gamut is reduced from 130% to 95% as the ambient light intensity increases from 0 lux to 2000 lux, it still covers most AdobeRGB color region and the image quality can be preserved. Under the direct sunlight (10 000 lux to 30 000 lux), the color gamut shrinks further, but still convers a great portion of AdobeRGB color region. Moreover, according to a psychophysical phenomenon called Helmholtz–Kohlrausch effect [69], [70], the highly saturated colors appear to be brighter than those with lower saturation, even they have the same luminance. QDs provide saturated light emission and therefore the colors remain more discernable under sunlight.

2) Suppressed Color Shift: Color shift is an important parameter describing the angular dependent color uniformity of a LCD system. References [8] and [71] provide a detailed explanation on color shift and the calculation methods. Fig. 19 depicts the color shift of film-compensated n-FFS and p-FFS using a white LED backlight [(a) and (c)] and a QD-LED backlight [(b) and (d)] in CIE 1976 diagram from different azimuthal incident angles at the full-bright gray level G255. From Fig. 19, we find that FFS with QD-LED exhibits a much weaker color shift than that using a white LED for all the RGB primaries. To quantitatively evaluate angular color uniformity, we calculate the color shift values ($\Delta u'v'$) of both n-FFS and p-FFS at different azimuthal angles, and the data are listed in Table II.

From Table II, film-compensated n-FFS and p-FFS modes have comparable $\Delta u'v'$ values in each category, which means their angular color uniformities are about the same. Detailed examination reveals the blue primary has a larger color shift than green and red within each family. In comparison with white LED, QD-LED shows much better angular color uniformity. This much weaker color shift originates from the narrower spectral bandwidth and less spectral overlapping of the QD-LED backlight.

Overall, QD-enhanced n-FFS shows attractive performances in following aspects: 1) high transmittance (98% @550 nm); 2) single gamma curve for RGB pixels; 3) wide viewing angle and negligible color shift; 4) extremely wide color gamut; and

TABLE II
CALCULATED $\Delta u'v'$ VALUES OF THE FILM COMPENSATED SINGLE DOMAIN $n-$ FFS AND $p-$ FFS LCDS WITH TWO DIFFERENT BACKLIGHTS. θ IS SCANNED FROM $-80°$ TO $80°$ AND ϕ IS SET AT $45°$ W.R.T. THE RUBBING ANGLE

		White LED	QD-LED ($\Delta\lambda$ = 10 nm)
	R	0.0092	5.67e-5
n-FFS	**G**	0.0103	1.03e-5
	B	0.0337	8.67e-5
	R	0.0101	6.29e-5
p-FFS	**G**	0.0105	1.25e-5
	B	0.0264	6.95e-5

TABLE III
CALCULATED $\Delta u'v'$ VALUES OF THE FILM-COMPENSATED SINGLE-DOMAIN AND MULTI-DOMAIN IPS-BPLC. θ IS SCANNED FROM $-80°$ TO $80°$ AND ϕ IS SET AT $45°$ W.R.T. THE RUBBING ANGLE

		Single domain	Multi domain
	R	0.0074	0.0009
IPS-BPLC	**G**	0.0073	0.0010
	B	0.0308	0.0062

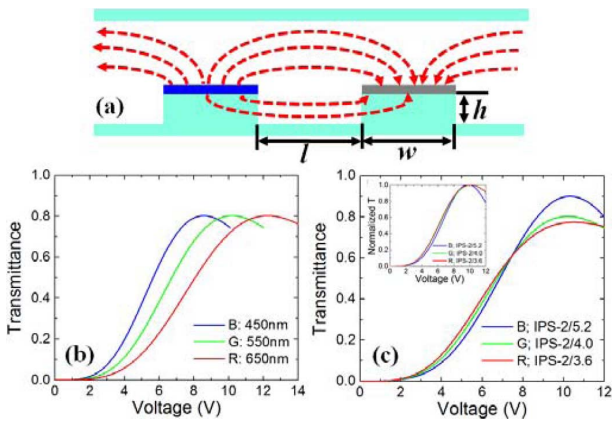

Fig. 20. (a) Cell structure of etched IPS-BPLC. (b) Simulated VT curves for RGB wavelengths. BPLC cell: etched IPS-2/4 with $h = 2.5$ μm and JC-BP06, and (c) Simulated VT curves for IPS-2/3.6 (R), IPS-2/4 (G), and IPS-2/5.2 (B) with $h = 2.5$ μm.

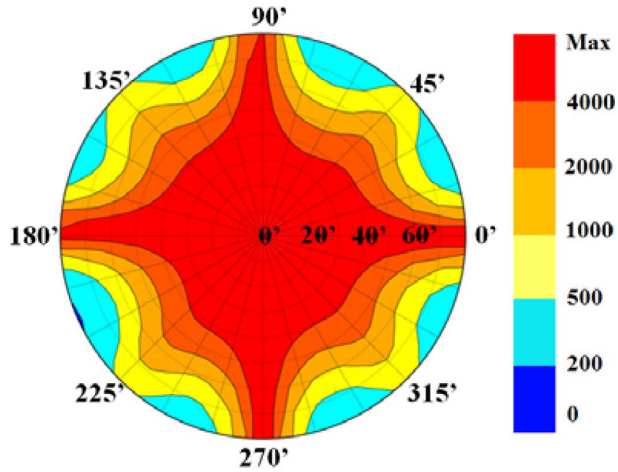

Fig. 21. Isocontrast contours of a four-domain BPLC with a biaxial compensation film.

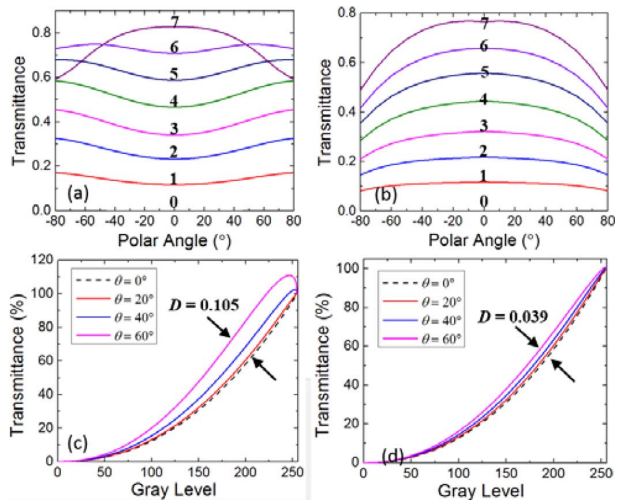

Fig. 22. Viewing angle dependent eight gray levels of film-compensated (a) single-domain etched IPS-BPLC and (b) multi-domain etched IPS-BPLC along the diagonal direction ($\phi = 45°$). Viewing angle dependence of gamma curves for film-compensated (c) single domain etched BPLC and (d) multi-domain etched BPLC along the diagonal direction ($\phi = 45°$).

5) excellent image quality at outdoor environment. Therefore, n-FFS is a strong contender for next-generation mobile displays.

C. QD-Enhanced IPS-BPLC

PS-BPLC has become an increasingly important technology for display and photonic applications [9]–[11]. It exhibits several attractive features, such as reasonably wide temperature range, submillisecond gray-to-gray response time, no need for alignment layer, optically isotropic voltage-off state, and large cell gap tolerance when an IPS cell is employed.

In terms of device configuration, both IPS [14], [15] and vertical field switching [72], [73] have been developed. IPS-BPLC is more appealing to general display applications because of its wide viewing angle and simple backlight system. Etched and protruded electrodes are two effective methods to reduce the operation voltage because of their deeper electric field penetration depth [15], [74]–[76]. Fig. 20(a) shows the device structure of an etched IPS-BPLC, where the electrodes are etched with $h = 2.5$ μm. For equally-spaced IPS structure with $l = 2$ μm and $w = 4$ μm, the on-state voltage of JC-BP06 is 12 V, 10 V and 9 V for RGB colors, respectively (Fig. 20(b)). We can intentionally vary the l/w ratios for RGB sub-pixels to achieve single gamma as Fig. 20(c) shows. The on-state voltage is $\sim$ 10 V, which can be conveniently driven by amorphous TFTs.

In the voltage-off state, PS-BPLC is optically isotropic. When sandwiched between crossed polarizers, light leakage would occur at an oblique angle in which the two crossed polarizers are no longer perpendicular to each other. To widen the viewing angle, we placed a half-wave biaxial film between the LC cell and the analyzer to reduce the off-axis light leakage in the dark state [23]. As Fig. 21 depicts, the viewing angle of film- compensated etched IPS-BPLC is wide and symmetric. The viewing zone with 200:1 isocontrast ratio covers over 85°. Comparing Figs. 15 and 21, IPS-BPLC exhibits a superior viewing angle to its nematic counterpart.

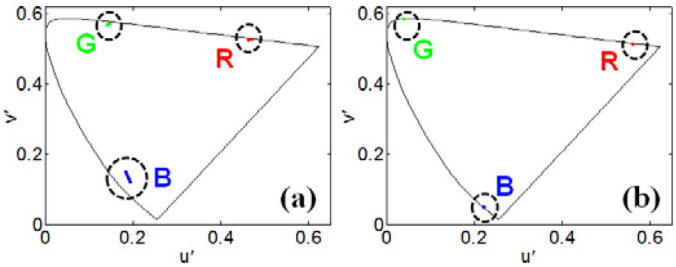

Fig. 23. Color shift of RGB primaries at 70° incident angle in the film-compensated BPLC: (a) Single domain structure, (b) Multi-domain structure. The backlight is white LED.

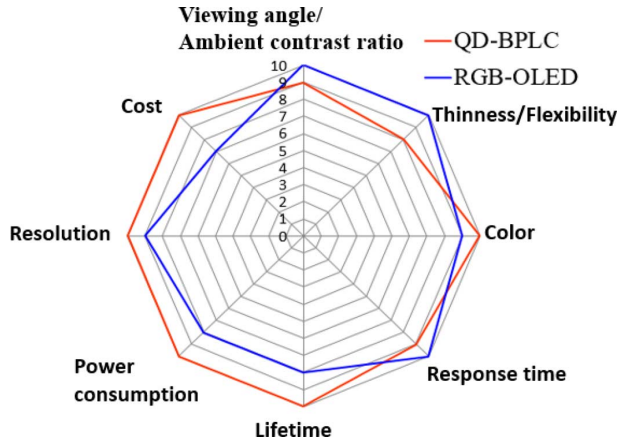

Fig. 24. Performance comparison of RGB OLED and QD enhanced BPLC.

Grayscale inversion is a problem for some single-domain LCDs at off-axis. Fig. 22(a) shows the viewing angle dependent eight gray levels for film-compensated single domain IPS-BPLC. Grayscale inversion exists from 6th gray level to 8th gray level. Comparing Fig. 22(a) with Fig. 16, we find single-domain IPS-BPLC exhibits a more severe grayscale inversion than single-domain nematic FFS. However, this drawback can be overcome by the multi-domain structure [77]. Single-domain IPS/FFS LCDs use stripe electrodes while multi-domain IPS/FFS LCDs use zigzag electrodes. As shown in Fig. 22(b), grayscale inversion is eliminated by the four-domain structure. Figs. 22(c), 22(d) also shows the viewing angle dependence of gamma curves of single/multi-domain IPS BPLC. The off-axis image distortion indices of single-domain and multi-domain IPS-BPLC are 0.105 and 0.039, respectively. From Fig. 22(d), the gamma curve of multi-domain BPLC is almost independent of viewing angles, which assures an excellent image quality for large off-axis viewing angle.

Multi-domain structure also helps to suppress color shift. Fig. 23 compares the color shift for single- and multi-domain BPLCs with white LED backlight. In multi-domain BPLC, the Kerr effect induced Δn is in the complementary directions between each subdomain, resulting in an even better and more uniformly compensated bright state. This can significantly suppress color shift. Blue primary has most severe color shift: for single domain IPS BPLC; its color shift is $\Delta u'v' = 0.0308$. For four domains, the color shift is reduced to $\Delta u'v' = 0.0062$. From Figs. 19 and 23, the color shift of BPLC and FFS is comparable but much less than that of TN and MVA.

The just noticeable color difference (JNCD) in CIE 1976 color space is 0.0040. So the color shift of multi-domain BPLC is quite acceptable. For commercial OLED devices, its color shift is $\Delta u'v' = 0.0229$ at 30° viewing angle. This color shift originates from the micro cavity effect. In comparison with OLED, BPLC shows much better off-axis color uniformity.

The most attractive feature of BPLC is its submillisecond gray-to-gray response time. Such a fast response time not only reduces motion blurs but also enables field sequential color (FSC) display [78], [79] with negligible color breakup. In FSC, the backlight sequentially emits RGB lights, and the LCD panel is synchronized with the backlight to display the required gray levels of each color. This color generation method does not require the conventional spatial color filters, therefore it offers 3X higher optical efficiency and resolution density.

QDs also improve the light efficiency and color performance for BPLC. It can be used for BPLC with color filters (normal mode) or FSC mode without color filters. In normal mode, QDs can be integrated either on-chip, on-cell or on-surface, and it functions similarly to its nematic counterpart. For FSC mode, the on-chip method should be used to only allow one color into the backlight system at a time. Current FSC LCDs use separated RGB LEDs as light source [27]. Although the quantum efficiency of blue and red semiconductor LEDs are pretty high, the availability of high efficiency green LED remains a challenge [80]. As a result, more green LEDs are needed in the backlight unit. This adds cost and energy consumption. Instead, green QD can be integrated with blue or UV LED to obtain highly efficient green emission. This concept is also known as color-by-blue displays [81]. It is also relatively easy to generate a specific color by changing the particle size of QDs than looking for a specific semiconductor material. Moreover, the radiative lifetime of QDs is $\sim$ 10 ns. Such a fast response time is more than sufficient for FSC operation.

Compared to nematic LCDs, BPLC possesses several attractive features: 1) submillisecond response time, 2) wide viewing angle and negligible color shift; 3) excellent dark state; 4) simpler fabrication process (no need for surface alignment); and 5) large cell gap tolerance and touch insensitivity. It is suitable for both mobile displays and TVs.

Fig. 24 compares the performance of QD-enhanced BPLC (QD-BPLC) with RGB OLEDs. QD-BPLC now has advantages in lifetime, power consumption, resolution density, color gamut, and cost. On the other hand, OLED still holds advantages in true black state (dark ambient), thin profile and flexibility. However, LCDs manifest the same level of ambient contrast ratio under the ambient light illumination [3], [5] and have less color shift. With local dimming technique, the dynamic contrast ratio [6] of LCDs can also be significantly improved. Slim LCD TV ($\sim$ 2 mm) and curved LCD TV are emerging in the market.

Motion blur was previously considered as a major drawback for TFT LCDs. Motion blur is often characterized by motion picture response time (MPRT) [82]. Unlike CRT which is an impulse-type display, both active matrix OLED and LCD are holding-type displays. Therefore, their MPRT is affected by material response time and sample-and-hold (S&H) effect [83].

According to a numerical analysis [82], when the material response time is reduced to submillisecond range, the MPRT is mainly determined by the S&H effect. For example, LG tested the MPRT for both LCD and OLED TVs [84]. Although OLED has much faster material response time (0.11 ms) than LCD (5.69 ms), their MPRT is comparable (6.65 ms for OLED vs. 7.56 ms for LCD) when driven at 120 Hz frame rate. BPLC has submillisecond material response time and, therefore, it can effectively mitigate the motion blur artifacts to a level similar to OLED. To further reduce MPRT, we have to increase the driving frequency to 240 Hz or higher. This could be a serious challenge for high resolution displays because the charging time for each TFT is greatly reduced. This problem is worse for the current-driven OLED as it requires more TFTs for each pixel.

V. Conclusion and Future Outlook

We have briefly reviewed the recent advances in quantum dots-enhanced LCDs for both mobile displays and TVs. QD backlight offers several advantages to LCDs, including: 1) highly saturated colors and wider color gamut ($\sim 120\%$ in CIE 1931 and $\sim 140\%$ in CIE 1976); 2) higher optical efficiency (up by 15%); 3) relaxed requirement for color filters; 4) perfect white point and mitigated color shift; and 5) retaining high contrast ratio under ambient light illumination. Two special QD LCDs are investigated in detail.

1) *QD-enhanced FFS:* It shows vivid colors, high optical efficiency, wide viewing angle, perfect white point, and improved ambient contrast ratio for mobile displays.
2) *QD-enhanced BPLC:* It reduces image blurs while keeping above-mentioned properties.

QD backlights are still evolving, and there are still several aspects that need further development, including: 1) To reduce QD toxicity and improve material quality of non-Cd QDs [50]. 2) To enhance the compatibility of QDs with silicone/ polymeric matrix so that QDs can be well dispersed without deteriorating photoluminescence and stability [85]. 3) To develop quantum rods with controllable emission direction/light polarization [86], [87] and QD platelets that offer highly saturated light emission [46], [47]. 4) To improve the optical packaging and material stability for on-chip method [88]. 5) To develop low cost, large panel QD films. Despite these technical challenges, QD-enhanced LCDs already show great advantages and potentials. The prime time for QD-enhanced LCDs is near.

The development of quantum dots together with blue phase LC add two strong wings to LCD industry, and make LCDs more appealing while competing with OLEDs. LCD can now match almost all the features that OLED can offer, except flexibility. Moreover, the cost of LCDs of all sizes is tough to beat by upstart technologies such as OLEDs. With dramatic improvements in color and response time, LCD is likely to continue its dominance. The prime time for QD-enhanced LCDs is around the corner.

Acknowledgment

The authors are indebted to Q. Hong, Y. Chen, Y. Liu, J. Yuan, and Y. Gao for valuable discussion.

References

[1] M. Schadt, "Milestone in the history of field-effect liquid crystal displays and materials," *Jpn. J. Appl. Phys.*, vol. 48, no. 3, p. 03B001, 2009.
[2] D. Barnes, "5.1: Invited paper: LCD or OLED: Who wins?," *SID Dig. Tech. Papers*, vol. 44, no. 1, pp. 26–27, 2013.
[3] J. H. Lee, K. H. Park, S. H. Kim, H. C. Choi, B. K. Kim, and Y. Yin, "5.3: Invited paper: AH-IPS, superb display for mobile device," *SID Dig. Tech. Papers*, vol. 44, no. 1, pp. 32–33, 2013.
[4] Y. Ukai, "5.2: Invited paper: TFT-LCDs as the future leading role in FPD," *SID Dig. Tech. Papers*, vol. 44, no. 1, pp. 28–31, 2013.
[5] R. M. Soneira, "Tablet display technology shoot-out," *Inf. Display*, vol. 29, no. 4, pp. 12–21, 2013.
[6] H. Chen, T. H. Ha, J. H. Sung, H. R. Kim, and B. H. Han, "Evaluation of LCD local-dimming-backlight system," *J. Soc. Inf. Displays*, vol. 18, no. 1, pp. 57–65, 2010.
[7] Q. Hong, T. X. Wu, X. Y. Zhu, R. B. Lu, and S. T. Wu, "Extraordinarily high-contrast and wide-view liquid-crystal displays," *Appl. Phys. Lett.*, vol. 86, no. 12, p. 121107, 2005.
[8] R. B. Lu, Q. Hong, S. T. Wu, K. H. Peng, and H. S. Hsieh, "Quantitative comparison of color performances between IPS and MVA LCDs," *J. Display Technol.*, vol. 2, no. 4, pp. 319–326, Dec. 2006.
[9] H. Kikuchi, M. Yokota, Y. Hisakado, H. Yang, and T. Kajiyama, "Polymer-stabilized liquid crystal blue phases," *Nat. Mater*, vol. 1, no. 1, pp. 64–68, 2002.
[10] Y. Chen and S.-T. Wu, "Recent advances on polymer-stabilized blue phase liquid crystal materials and devices," *J. Appl. Polymer Sci.*, p. 40556, 2014.
[11] J. Yan, L. H. Rao, M. Z. Jiao, Y. Li, H. C. Cheng, and S. T. Wu, "Polymer-stabilized optically isotropic liquid crystals for next-generation display and photonics applications," *J. Mater. Chem.*, vol. 21, no. 22, pp. 7870–7877, 2011.
[12] Y. Hirakata, D. Kubota, A. Yamashita, T. Ishitani, T. Nishi, H. Miyake, H. Miyairi, J. Koyama, S. Yamazaki, T. Cho, and M. Sakakura, "A novel field-sequential blue-phase-mode AMLCD," *J. Soc. Inf. Displays*, vol. 20, no. 1, pp. 38–46, 2012.
[13] Y. F. Liu, Y. F. Lan, H. X. Zhang, R. D. Zhu, D. M. Xu, C. Y. Tsai, J. K. Lu, N. Sugiura, Y. C. Lin, and S. T. Wu, "Optical rotatory power of polymer-stabilized blue phase liquid crystals," *Appl. Phys. Lett.*, vol. 102, no. 13, p. 131102, 2013.
[14] L. H. Rao, Z. B. Ge, S. T. Wu, and S. H. Lee, "Low voltage blue-phase liquid crystal displays," *Appl. Phys. Lett.*, vol. 95, no. 23, p. 231101, 2009.
[15] D. M. Xu, Y. Chen, Y. F. Liu, and S. T. Wu, "Refraction effect in an in-plane-switching blue phase liquid crystal cell," *Opt. Express*, vol. 21, no. 21, pp. 24721–24735, 2013.
[16] K. M. Chen, S. Gauza, H. Q. Xianyu, and S. T. Wu, "Hysteresis effects in blue-phase liquid crystals," *J. Display Technol.*, vol. 6, no. 8, pp. 318–322, Aug. 2010.
[17] J. Yan, H. C. Cheng, S. Gauza, Y. Li, M. Z. Jiao, L. H. Rao, and S. T. Wu, "Extended Kerr effect of polymer-stabilized blue-phase liquid crystals," *Appl. Phys. Lett.*, vol. 96, no. 7, p. 071105, 2010.
[18] H. Y. Kim, S. M. Seen, Y. H. Jeong, G. H. Kim, T. Y. Eom, S. Y. Kim, Y. J. Lim, and S. H. Lee, "P-164: pressure-resistant characteristic of fringe-field switching (FFS) mode depending on the distance between pixel electrodes," *SID Dig. Tech. Papers*, vol. 36, no. 1, pp. 325–327, 2005.
[19] J. Lim, Z. Zhang, F. Yang, X. Zuo, R. Yang, Y. Ko, and H. Jung, "P-213L: late-news poster: Optimization of high-aperture-ratio fringe-field-switching pressure-resistance characteristic for touch-screen display," *SID Dig. Tech. Papers*, vol. 42, no. 1, pp. 1650–1653, 2011.
[20] S. H. Lee, S. S. Bhattacharyya, H. S. Jin, and K. U. Jeong, "Devices and materials for high-performance mobile liquid crystal displays," *J. Mater. Chem.*, vol. 22, no. 24, pp. 11893–11903, 2012.
[21] S. H. Lee, S. L. Lee, and H. Y. Kim, "Electro-optic characteristics and switching principle of a nematic liquid crystal cell controlled by fringe-field switching," *Appl. Phys. Lett.*, vol. 73, no. 20, pp. 2881–2883, 1998.
[22] S. H. Lee, S. M. Kim, and S.-T. Wu, "Review paper: Emerging vertical-alignment liquid-crystal technology associated with surface modification using UV-curable monomer," *J. Soc. Inf. Disp.*, vol. 17, no. 7, pp. 551–559, 2009.
[23] D. K. Yang and S. T. Wu, *Fundamentals of Liquid Crystal Devices*. Hoboken, NJ, USA: Wiley, 2006.

[24] S. H. Ji, H. C. Lee, J. M. Yoon, J. C. Lim, M. Jun, and E. Yeo, "P.91: adobe RGB LCD monitor with 3 primary colors by deep green color filter technology," *SID Dig. Tech. Papers*, vol. 44, no. 1, pp. 1332–1334, 2013.

[25] R. J. Xie, N. Hirosaki, and T. Takeda, "Wide color gamut backlight for liquid crystal displays using three-band phosphor-converted white light-emitting diodes," *Appl. Phys.Express*, vol. 2, p. 022401, 2009.

[26] R. B. Lu, S. Gauza, and S. T. Wu, "LED-lit LCD TVs," *Mol. Cryst. Liq. Cryst.*, vol. 488, pp. 246–259, 2008.

[27] M. Anandan, "Progress of LED backlights for LCDs," *J. Soc. Inf. Disp.*, vol. 16, no. 2, pp. 287–310, 2008.

[28] S. Kim, S. H. Im, and S. W. Kim, "Performance of light-emitting-diode based on quantum dots," *Nanoscale*, vol. 5, no. 12, pp. 5205–5214, 2013.

[29] J. Lim, W. K. Bae, J. Kwak, S. Lee, C. Lee, and K. Char, "Perspective on synthesis, device structures, and printing processes for quantum dot displays," *Opt. Mater. Express*, vol. 2, no. 5, pp. 594–628, 2012.

[30] Y. Shirasaki, G. J. Supran, M. G. Bawendi, and V. Bulovic, "Emergence of colloidal quantum-dot light-emitting technologies," *Nat. Photonics*, vol. 7, no. 1, pp. 13–23, 2013.

[31] L. Qian, Y. Zheng, J. G. Xue, and P. H. Holloway, "Stable and efficient quantum-dot light-emitting diodes based on solution-processed multilayer structures," *Nat. Photon.*, vol. 5, no. 9, pp. 543–548, 2011.

[32] Q. Sun, Y. A. Wang, L. S. Li, D. Y. Wang, T. Zhu, J. Xu, C. H. Yang, and Y. F. Li, "Bright, multicoloured light-emitting diodes based on quantum dots," *Nat. Photon.*, vol. 1, no. 12, pp. 717–722, 2007.

[33] E. Jang, S. Jun, H. Jang, J. Lim, B. Kim, and Y. Kim, "White-Light-Emitting diodes with quantum dot color converters for display backlights," *Adv. Mater.*, vol. 22, no. 28, pp. 3076–3080, 2010.

[34] S. Coe-Sullivanz, W. Liu, P. Allen, and J. S. Steckel, "Quantum dots for LED downconversion in display applications," *J. Solid State Sci. Technol*, vol. 2, no. 2, pp. 3026–3030, 2013.

[35] J. Chen, V. Hardev, J. Hartlove, J. Hofler, and E. Lee, "66.1: Distinguised paper: A high-efficiency wide-color-gamut solid-state backlight system for LCDs using quantum dot enhancement film," *SID Dig. Tech. Papers*, vol. 43, no. 1, pp. 895–896, 2012.

[36] C. B. J. Steckel, W. Liu, J. Xi, C. Hamilton, and S. Coe-Sullivan, "Quantum dots: The ultimate down-conversion material for LCDs," *SID Dig. Tech. Papers*, vol. 45, 2014.

[37] J. S. Steckel, R. Colby, W. Liu, K. Hutchinson, C. Breen, J. Ritter, and S. Coe-Sullivan, "68.1: Invited paper: Quantum dot manufacturing requirements for the high volume LCD market," *SID Dig. Tech. Papers*, vol. 44, no. 1, pp. 943–945, 2013.

[38] J. Chen, V. Hardev, and J. Yurek, "Quantum-Dot displays: Giving LCDs a competitive edge through color," *Inf. Display*, vol. 29, no. 1, pp. 12–17, 2013.

[39] Y. Chen, Z. Luo, F. Peng, and S. T. Wu, "Fringe-field switching with a negative dielectric anisotropy liquid crystal," *J. Display Technol.*, vol. 9, no. 2, pp. 74–77, Feb. 2013.

[40] Y. Chen, F. Peng, T. Yamaguchi, X. Song, and S. T. Wu, "High performance negative dielectric anisotropy liquid crystals for display applications," *Crystals*, vol. 3, no. 3, pp. 483–503, 2013.

[41] H. Choi, J. H. Yeo, and G. D. Lee, "Zig-zag electrode pattern for high brightness in a super in-plane-switching liquid-crystal cell," *J. Soc. Info. Disp.*, vol. 17, no. 10, pp. 827–831, 2009.

[42] H. J. Yun, M. H. Jo, I. W. Jang, S. H. Lee, S. H. Ahn, and H. J. Hur, "Achieving high light efficiency and fast response time in fringe field switching mode using a liquid crystal with negative dielectric anisotropy," *Liq. Cryst.*, vol. 39, no. 9, pp. 1141–1148, 2012.

[43] H. Hong, H. Shin, and I. Chung, "In-plane switching technology for liquid crystal display television," *J. Display Technol.*, vol. 3, no. 4, pp. 361–370, 2007.

[44] A. M. Smith and S. M. Nie, "Semiconductor nanocrystals: Structure, properties, and band gap engineering," *Accounts Chem Res*, vol. 43, no. 2, pp. 190–200, 2010.

[45] L. Brus, "Electronic wave-functions in semiconductor clusters—experiment and theory," *J. Phys. Chem.*, vol. 90, no. 12, pp. 2555–2560, 1986.

[46] S. Ithurria, G. Bousquet, and B. Dubertret, "Continuous transition from 3D to 1D confinement observed during the formation of cdse nanoplatelets," *J. Amer. Chem. Soc.*, vol. 133, no. 9, pp. 3070–3077, 2011.

[47] S. Ithurria and B. Dubertret, "Quasi 2D colloidal CdSe platelets with thicknesses controlled at the atomic level," *J. Amer. Chem. Soc.*, vol. 130, no. 49, pp. 16504–16505, 2008.

[48] P. Reiss, M. Protiere, and L. Li, "Core/shell semiconductor nanocrystals," *Small*, vol. 5, no. 2, pp. 154–168, 2009.

[49] M. Green, "The nature of quantum dot capping ligands," *J. Mater. Chem.*, vol. 20, no. 28, pp. 5797–5809, 2010.

[50] M. J. Anc, N. L. Pickett, N. C. Gresty, J. A. Harris, and K. C. Mishra, "Progress in Non-Cd quantum dot development for lighting applications," *J. Solid State Sci. Technol*, vol. 2, no. 2, pp. R3071–R3082, 2013.

[51] X. Y. Yang, D. W. Zhao, K. S. Leck, S. T. Tan, Y. X. Tang, J. L. Zhao, H. V. Demir, and X. W. Sun, "Full visible range covering InP/ZnS nanocrystals with high photometric performance and their application to white quantum dot light-emitting diodes," *Adv. Mater.*, vol. 24, no. 30, pp. 4180–4185, 2012.

[52] H. Kim, J. Y. Han, D. S. Kang, S. W. Kim, D. S. Jang, M. Suh, A. Kirakosyan, and D. Y. Jeon, "Characteristics of CuInS2/ZnS quantum dots and its application on LED," *J. Cryst. Growth*, vol. 326, no. 1, pp. 90–93, 2011.

[53] H. Menkara, R. A. Gilstrap, T. Morris, M. Minkara, B. K. Wagner, and C. J. Summers, "Development of nanophosphors for light emitting diodes," *Opt. Express*, vol. 19, no. 14, pp. A972–A981, 2011.

[54] H.-M. Kim and J. Jang, "High-Efficiency inverted quantum-dot light emitting diodes for displays," *SID Dig. Tech. Papers*, vol. 45, 2014.

[55] S. Kobayashi, S. Mikoshiba, and S. Lim, *LCD Backlights*. Hoboken, NJ, USA: Wiley, 2009.

[56] J. H. Lee, D. N. Liu, and S. T. Wu, *Introduction to Flat Panel Displays*. Hoboken, NJ: Wiley, 2008.

[57] G. Wyszecki and W. Stiles, *Color Science—Concepts and Methods, Quantitative Data and Formulate*, 2nd ed. New York: Wiley, 1982.

[58] Z. Luo, Y. Chen, and S. T. Wu, "Wide color gamut LCD with a quantum dot backlight," *Opt. Express*, vol. 21, no. 22, pp. 26269–26284, 2013.

[59] M. Reyes-Sierra and C. A. C. Coello, "Multi-objective particle swarm optimizers: A survey of the state-of-the-art," *Int. J. Comput. Intell. Res*, vol. 2, no. 3, pp. 287–308, 2006.

[60] Z. Luo and S. T. Wu, "A spatiotemporal four-primary color LCD with quantum dots," *J. Display Technol.*, vol. 10, no. 5, pp. 367–372, May 2014.

[61] M. Schadt and W. Helfrich, "Voltage-Dependent optical activity of a twisted nematic liquid crystal," *Appl. Phys. Lett.*, vol. 18, no. 4, p. 127, 1971.

[62] A. Takeda, S. Kataoka, T. Sasaki, H. Chida, H. Tsuda, K. Ohmuro, T. Sasabayashi, Y. Koike, and K. Okamoto, "41.1: a super-high image quality multi-domain vertical alignment LCD by new rubbing-less technology," *SID Dig. Tech. Papers*, vol. 29, no. 1, pp. 1077–1080, 1998.

[63] Y. Chen, J. Yan, J. Sun, S. T. Wu, X. Liang, S. H. Liu, P. J. Hsieh, K. L. Cheng, and J. W. Shiu, "A microsecond-response polymer-stabilized blue phase liquid crystal," *Appl. Phys. Lett.*, vol. 99, no. 20, p. 201105, 2011.

[64] L. M. Blinov and V. G. Chigrinov, *Electrooptic Effects in Liquid Crystal Materials*. New York: Springer-Verlag, 1994.

[65] R. B. Lu, X. Y. Zhu, S. T. Wu, Q. Hong, and T. X. Wu, "Ultrawide-View liquid crystal displays," *J. Display Technol.*, vol. 1, no. 1, pp. 3–14, 2005.

[66] X. Zhu, Z. Ge, and S. T. Wu, "Analytical solutions for uniaxial-film-compensated wide-view liquid crystal displays," *J. Display Technol.*, vol. 2, no. 1, pp. 2–20, Mar. 2006.

[67] S. S. Kim, B. H. Berkeley, K. H. Kim, and J. K. Song, "New technologies for advanced LCD-TV performance," *J. Soc. Inf. Displays*, vol. 12, no. 4, pp. 353–359, 2004.

[68] J. H. Lee, X. Y. Zhu, Y. H. Lin, W. K. Choi, T. C. Lin, S. C. Hsu, H. Y. Lin, and S. T. Wu, "High ambient-contrast-ratio display using tandem reflective liquid crystal display and organic light-emitting device," *Opt. Express*, vol. 13, no. 23, pp. 9431–9438, 2005.

[69] R. L. Donofrio, "Review paper: The Helmholtz–Kohlrausch effect," *J. Soc. Inf. Disp.*, vol. 19, no. 10, pp. 658–664, 2011.

[70] P. K. Kaiser, "The Helmholtz–Kohlrausch effect," *Color Res. Appl.*, vol. 10, no. 3, p. 187, 1985.

[71] R. Lu, Q. Hong, Z. B. Ge, and S. T. Wu, "Color shift reduction of a multi-domain IPS-LCD using RGB-LED backlight," *Opt. Express*, vol. 14, no. 13, pp. 6243–6252, 2006.

[72] H. C. Cheng, J. Yan, T. Ishinabe, C. H. Lin, K. H. Liu, and S. T. Wu, "Wide-View vertical field switching blue-phase LCD," *J. Display Technol.*, vol. 8, no. 11, pp. 627–633, Nov. 2012.

[73] H. C. Cheng, J. Yan, T. Ishinabe, N. Sugiura, C. Y. Liu, T. H. Huang, C. Y. Tsai, C. H. Lin, and S. T. Wu, "Blue-Phase liquid crystal displays with vertical field switching," *J. Display Technol.*, vol. 8, no. 2, pp. 98–103, Feb. 2012.

[74] L. H. Rao, H. C. Cheng, and S. T. Wu, "Low voltage blue-phase LCDs with double-penetrating fringe fields," *J. Display Technol.*, vol. 6, no. 8, pp. 287–289, 2010.
[75] L. H. Rao, Z. B. Ge, and S. T. Wu, "Zigzag electrodes for suppressing the color shift of Kerr effect-based liquid crystal displays," *J. Display Technol.*, vol. 6, no. 4, pp. 115–120, Apr. 2010.
[76] C.-Y. Tsai, T.-J. Tseng, L.-Y. Wang, F.-C. Yu, Y.-F. Lan, P.-J. Huang, S.-Y. Lin, K.-M. Chen, B.-S. Tseng, C.-W. Kuo, C.-H. Lin, J.-K. Lu, and N. Sugiura, "17.1: Invited paper: Polymer-stabilized blue phase liquid crystal displays applying novel groove cell structure," *SID Dig. Tech. Papers*, vol. 44, no. 1, pp. 182–183, 2013.
[77] L. Rao, Z. Ge, and S. T. Wu, "Zigzag electrodes for suppressing the color shift of Kerr effect-based liquid crystal displays," *J. Display Technol.*, vol. 6, no. 4, pp. 115–120, Apr. 2010.
[78] C. H. Chen, F. C. Lin, Y. T. Hsu, Y. P. Huang, and H. P. D. Shieh, "A field sequential color LCD based on color fields arrangement for color breakup and flicker reduction," *J. Display Technol.*, vol. 5, no. 1-3, pp. 34–39, 2009.
[79] T. Ishinabe, K. Wako, K. Sekiya, T. Kishimoto, T. Miyashita, and T. Uchida, "High-performance OCB-mode field-sequential-color LCD," *J. Soc. Inf. Displays*, vol. 16, no. 2, pp. 251–256, 2008.
[80] M. R. Krames, O. B. Shchekin, R. Mueller-Mach, G. O. Mueller, L. Zhou, G. Harbers, and M. G. Craford, "Status and future of high-power light-emitting diodes for solid-state lighting," *J. Display Technol.*, vol. 3, no. 2, pp. 160–175, Jun. 2007.
[81] J. H. Oh, K.-H. Lee, H. C. Yoon, H. Yang, and Y. R. Do, "Color-by-blue display using blue quantum dot light-emitting diodes and green/red color converting phosphors," *Opt. Express*, vol. 22, no. S2, pp. A511–A520, 2014.
[82] Y. Igarashi, T. Yamamoto, Y. Tanaka, J. Someya, Y. Nakakura, M. Yamakawa, Y. Nishida, and T. Kurita, "43.3: summary of moving picture response time (MPRT) and futures," *SID Dig. Tech. Papers*, vol. 35, no. 1, pp. 1262–1265, 2004.
[83] Y. Zhang, X. Li, Y. Xu, Y. Shi, W. Song, and W. Lei, "Motion-blur characterization with simulation method for mobile LCDs," *J. Soc. Inf. Disp.*, vol. 16, no. 11, pp. 1115–1123, 2008.
[84] J.-K. Yoon, E.-M. Park, J.-S. Son, H.-W. Shin, H.-E. Kim, M. Yee, H.-G. Kim, C.-H. Oh, and B.-C. Ahn, "27.2: the study of picture quality of OLED TV with WRGB OLEDs structure," *SID Dig. Tech. Papers*, vol. 44, no. 1, pp. 326–329, 2013.
[85] H. V. Demir, S. Nizamoglu, T. Erdem, E. Mutlugun, N. Gaponik, and A. Eychmuller, "Quantum dot integrated LEDs using photonic and excitonic color conversion," *Nano Today*, vol. 6, no. 6, pp. 632–647, 2011.
[86] J. T. Hu, L. S. Li, W. D. Yang, L. Manna, L. W. Wang, and A. P. Alivisatos, "Linearly polarized emission from colloidal semiconductor quantum rods," *Sci.*, vol. 292, no. 5524, pp. 2060–2063, 2001.
[87] A. Sitt, A. Salant, G. Menagen, and U. Banin, "Highly emissive nano rod-in-rod heterostructures with strong linear polarization," *Nano Lett.*, vol. 11, no. 5, pp. 2054–2060, 2011.
[88] J. Kurtin, N. Puetz, B. Theobald, N. Stott, and J. Osinski, "12.5: quantum dots for high-color-gamut LCDs using an on-chip LED solution," *SID Dig. Tech. Papers*, 2014.

Zhenyue Luo received the B.S. and M.S. degrees in optics from Zhejiang University, Hangzhou, China, in 2007 and 2010, respectively.

Since 2010, he has been a research assistant in Photonics and Display Group, University of Central Florida, Orlando, FL, USA. His current research focuses on backlight design and liquid crystal devices.

Daming Xu received the B.S. degree in information engineering from Southeast University, Nanjing, China, in 2011, and is currently working toward the Ph.D. degree in the College of Optics and Photonics, University of Central Florida, Orlando, FL, USA. His current research focuses on fast-response nematic liquid crystal devices and blue phase liquid crystal displays.

Mr. Xu is the recipient of SID Distinguished Student Paper Award for two years in a row (2013 and 2014).

Shin-Tson Wu (M'98–SM'99–F'04) received the B.S. degree in physics from National Taiwan University, Taipei, Taiwan, and the Ph.D. degree from the University of Southern California, Los Angeles, CA, USA.

He is a Pegasus professor at College of Optics and Photonics, University of Central Florida, Orlando, Orlando, FL, USA.

Dr. Wu is the recipient of Esther Hoffman Beller Medal (2014), SID Slottow-Owaki prize (2011), OSA Joseph Fraunhofer award (2010), SPIE G. G. Stokes award (2008), and SID Jan Rajchman prize (2008). He was the founding Editor-in-Chief of IEEE/OSA JOURNAL OF DISPLAY TECHNOLOGY. He is a Charter Fellow of the National Academy of Inventors, a Fellow of the Society of Information Display (SID), Optical Society of America (OSA), and SPIE.